

Finite Element Analysis to model ischemia experienced in the development of device related pressure ulcers.

LEUNG, Isaac PH, FLEMING, Leigh <<http://orcid.org/0000-0002-6962-8686>>, WALTON, Karl, SIMON, Barrans and OUSEY, Karen

Available from Sheffield Hallam University Research Archive (SHURA) at:

<http://shura.shu.ac.uk/24525/>

This document is the author deposited version. You are advised to consult the publisher's version if you wish to cite from it.

Published version

LEUNG, Isaac PH, FLEMING, Leigh, WALTON, Karl, SIMON, Barrans and OUSEY, Karen (2019). Finite Element Analysis to model ischemia experienced in the development of device related pressure ulcers. Proceedings of the Institution of Mechanical Engineers, Part H: Journal of Engineering in Medicine.

Copyright and re-use policy

See <http://shura.shu.ac.uk/information.html>

Finite Element Analysis to model ischemia experienced in the development of device related pressure ulcers.

*Isaac P. H. Leung^{*1}, Leigh T. Fleming², Karl Walton¹, Simon M. Barrans³, Karen Ousey⁴*

1. Centre for Precision Technologies (CPT), School of Computing and Engineering, University of Huddersfield

2. Materials Engineering Research Institute (MERI), Department of Engineering and Mathematics, Sheffield Hallam University, UK

3. Turbocharger Research Institute, University of Huddersfield, UK

4. Institute of Skin Integrity and Infection Prevention, University of Huddersfield, UK

**Corresponding author, Email: Pakhung.leung@hud.ac.uk*

Abstract

Pressure ulcers are a common occurrence of damage to skin. Severity ranges from slightly discoloured skin to full thickness tissue damage which can be fatal in some cases. Engineering effort, typically developing computational models had made significant progress in the understanding and demonstration of the formation mechanism of pressure ulcers with the aetiology of excessive stress however relatively limited attempts had been made to develop relevant models for pressure ulcers caused by ischemia. The aim of this paper is to present evidence of a computational model developed to simulate ischemic pressure ulcer formation and demonstrate the established relationship between the computational data and the acquired clinically relevant experimental data by utilising laser Doppler velocimetry. The application of the presented computational model and the established relationship allows the evaluation of the effect of a mechanical loading to the cutaneous blood flow velocity which is a step closing to understand and evaluate a mechanical load to the formation of pressure ulcers caused by ischemia.

Keywords: Pressure ulcer, finite element method, ischemia, cutaneous blood flow, computational model

Introduction

Skin is a large and multifunctional organ of human body which acts as a barrier to prevent harmful pathogens and chemicals from entering the body, it regulates body temperature, and also absorbs shock (1). A pressure ulcer (PU) can be described as localised skin damage which is a significant, health risk to patients, in most serious cases can be fatal through complications such as infection due to loss of skin integrity as a barrier and in most occurrences reduces the quality of life outcomes for patients. There is also a serious financial burden to health care providers and funding bodies. A PU is officially defined as: "A PU is localised damage to the skin and/or underlying tissue, usually over a bony prominence (or related to a medical or other device), resulting from sustained pressure (including pressure associated with shear). The damage can be present as intact skin or an open ulcer and may be painful". (NHSi, 2018). The financial and social burden of pressure ulceration is a global challenge, with the Department of Health & Human Services of the United States, stating there are 2.5 million patients suffering from PUs and 60,000 patients dead as a direct result of a PU with more than 17,000 lawsuits which are PU related each year (2). The prevalence rate of PUs for 186,000 patients from a range of healthcare settings in one large cohort study was reported as 4.36% from July 2017 to July 2018 (NHS Safety Thermometer)(3). PUs are categorised into four different stages by the wound depth. Category I PUs present as discoloration with intact skin, Category II PUs show presence of an open wound where only superficial layers are damaged. Category III and IV PUs result in full thickness skin loss and tissue loss respectively including muscle

and tendons. There are two additional categories defined by the European Pressure Ulcer Advisory Panel and National Pressure Ulcer Advisory Panels from the United States of America (4); 'Unstageable' is an extra stage referring to those PUs which are hard to be evaluated and 'deep tissue injury' referring to those which are damaged in deep layers with intact superficial layers. The National Health Service (NHS) in the UK spends £ 3.8 million everyday on the treatment of PUs (5). It was estimated that PUs cost £180-321 million (0.4-0.8% of health spending) in 1993, increasing to £1.43-2.14 billion annually (4.1% of the NHS expenditure) in 2000 (6). The time cost for the clinicians to treat the PUs accounts for 90% of the costs and 96% of the cost for stage I and II PUs (7). It is evident from these statistics, that a reduction in the prevalence of PUs would result in improved outcomes for patients, and a decrease in resource burden, both financial and time for the NHS and other private providers of care.

The factors affecting PU development are well documented. A range of factors can cause formation of PUs including friction, shear, pressure and microclimate of the skin surface (8, 9). Both excessive distortion and shear within the deep tissue and ischemia at the superficial layers of skin are the known causes of the development of PUs (10). Excessive distortion and shear at the deep tissue usually cause deep tissue injury (11-13). The superficial layers of skin are usually intact but there is discolouration of the surface of the skin, this can result in a category III or IV PU once the superficial layers of skin break down (10). Ischemia, "an inadequate flow of blood to a part of the body, caused by constriction or blockage of blood vessels supplying it", (14) on the skin is usually caused by prolonged application of pressure with or without friction which is often the case for medical device related PUs (MDRPU) (15-17). Although PUs caused by ischemia are usually category I or II, they contribute to a significant portion of the total prevalence of PUs. Indeed a study by Black in 2010 confirmed that over one third of the total prevalence of PUs was related to medical devices and among the total incidents of MEDPU, 67% of those are in Category I and II which are superficial (18). The nature of PUs caused by medical devices is most likely to be caused by ischemia, this is due to the low pressure magnitude coupled with a prolonged contact between the device and skin.

Different computational models have been developed to understand and demonstrate the internal conditions of human bodies when different mechanical loadings are applied to skin including pressure, friction and shear. A 3-D finite element model for human buttocks developed by Makhsous (13) indicated the internal stress and pressure among different soft tissue validated by utilising magnetic resonance (MRI) imaging. A real-time subject-specific finite element (FE) model was developed by Linder-Ganz (19) to demonstrate that the average peak gluteal stress was 3 to 5 times higher in the subjects with spinal cord injury than healthy control participants. A model of a subject's buttock, foam cushion and air-cell-based (ACB) cushions were used by Levy (20) to demonstrate that 57% greater immersion and 4 orders-of magnitude lower for stress was gained by sitting on ACB cushion. Luboz in 2017 developed a finite element reduced order subject-specific buttock model which approximated the internal strain of patient in real time which could be adopted for interactive precaution of deep tissue injury or Category III and IV PU warning tool (21). These models were capable of demonstrating the formation mechanism of PUs relating to internal stress and strain however they are incapable of showing any relationship with restriction of blood flow. A wide study in literature was conducted by Savonnet *et. al.* on different FE models which highlighted the fact that most of the FE models focused on contact pressure and internal stress (22). The first attempt of understanding the effect of pressure to cutaneous blood vessels was found in Leung's study which highlighted that the interface pressure between the volunteers and the supporting surface was still one of the key factors for the input of the finite element (FE) model simulation (23). Even though the interface pressure may not be able to reflect the internal stress experienced by the muscle and other soft tissue, it is still a good parameter for indicating the pressure experienced by superficial layers of

skin. The study concluded that interface pressure affected the cross-sectional area reductions of the cutaneous blood vessels. The study established that the combined effects of pressure and friction from volunteers in sitting posture caused the cross-sectional area of blood vessels to reduce by 15.0% to 19.3% depending on the locations of blood vessels (23).

The previous model developed by Leung *et. al.* in 2017 was capable of demonstrating the cross-sectional area change of the cutaneous blood vessels (23). Though the model was restricted in demonstration of single direction friction because of the two mirror boundary conditions applied and also, there was still a lack of relationship between the percentage change of the cross-sectional area change of the cutaneous blood vessels from the computational simulations and the actual clinical-relevant change of skin by applying pressure. This paper presents results in an attempts to demonstrate a relationship between the computational model (FE) and clinically relevant experimental data which is obtained by utilising Laser Doppler Velocimetry on six healthy volunteers. Through this initial sample the primary aim is to prove the feasibility of the method and gather data from a pilot study on cutaneous blood flow.

This seeks to address the gap in knowledge of developing effective computational tools and related experimental results on the reduction in area of cutaneous blood vessels and the effect of cutaneous blood flow caused by mechanical loads. The presented model serves to evaluate the change in the cross-sectional area and the experimental results proves the feasibility of the methods in understanding the change in cutaneous blood flow velocity.

Method

The previous model (23) demonstrated the effect of the mechanical loading (pressure and friction) to the cutaneous blood vessels at the centre of the loading area of a volunteer sitting on a foam supporting surface. For the majority of the cutaneous blood vessels, it would not be located at the exact centre of the loading area and friction would be in single direction as the friction was in radially outward direction illustrated in the model developed in 2017. However, single direction friction was not able to be applied in the model presented in 2017 because of the two applied mirror boundary conditions. The model presented in this study, hence, has been developed to allow the application of single direction of friction and the relationship between the computational data from the FEA simulation and the acquired clinically related data has been established. Abaqus CAE 6.14 was used for development of the proposed model.

Feature of the Model

The current model was developed in micrometre scale as this gives the appropriate dimensions to represent the key interest of the model (cutaneous blood vessels). The model was a halved circle with the diameter of 41,200 μm . The model consisted of four layers in vertical direction representing three cutaneous layers including the epidermis, dermis and hypodermis. The extra layer for the current model was the stratum corneum which is part of the epidermis as shown in Figure 1 (a). In this model it was a separate layer because of its significant difference in mechanical properties compared to the rest of the epidermis layer. The presented model consisted of 10 radial sections which were developed to ensure different mesh sizes could be adopted for different sections as shown in Figure 1 (b). The model aims to relate the computational model to a set of acquire experimental data to establish a relationship between the cutaneous blood flow velocity and the

reduction in the cross-sectional area of cutaneous blood vessels. Hence, the study has been restricted to the cutaneous layers. The computational model would not be directly comparable to the anatomical location where the laser Doppler measurement is conducted if the deeper tissues i.e. muscles are involved, this is due to the limitations of flow measurement with the laser doppler method.

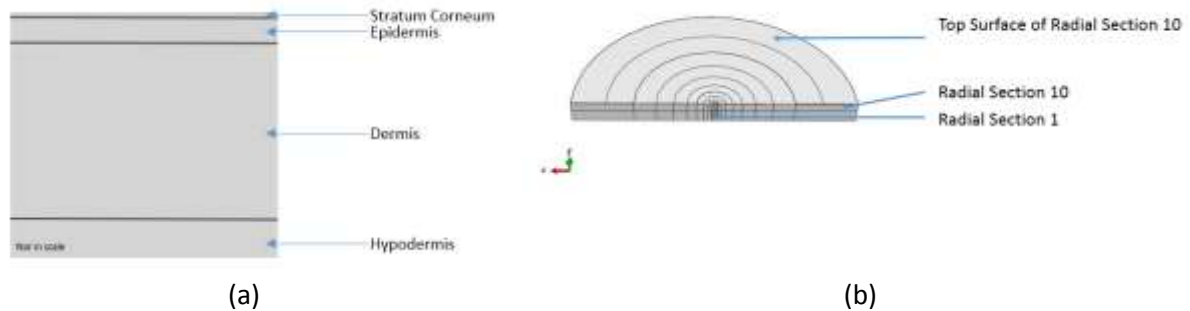


Figure 1 (a) Vertical Layers of the Model (b) Radial Sections

Internal Features of the Model

The primary interest of the model was the cutaneous blood vessels located at the first radial section at the dermis and hypodermis layers. These cutaneous blood vessels were represented by hollow circular tubes at the respective vertical layers as shown in Figure 2 (a). The deformation of the cutaneous layers resulting in the change in the cross-sectional area was the main interest of the study. There were nine horizontal cutaneous blood vessels and six sections of interest were located on each of the horizontal cutaneous blood vessels as shown in Figure 2 (b). The change in the cross-sectional area of the cutaneous blood vessels were calculated by analysing the deformation of the nodes on these sections of interest. All the cutaneous blood vessels with $15\mu\text{m}$ diameters represented the blood vessels that were slightly larger than capillaries. Two of the nine horizontal blood vessels were located at the dermis layers including one near the epidermis-dermis intersections and another one near the dermis-hypodermis intersections this was in agreement with the work by Démarchez (24). The remaining seven horizontal cutaneous blood vessels were located at the hypodermis layer as the hypodermis layers is known to be highly vascularised (25) but exact vertical locations were yet to be determined.

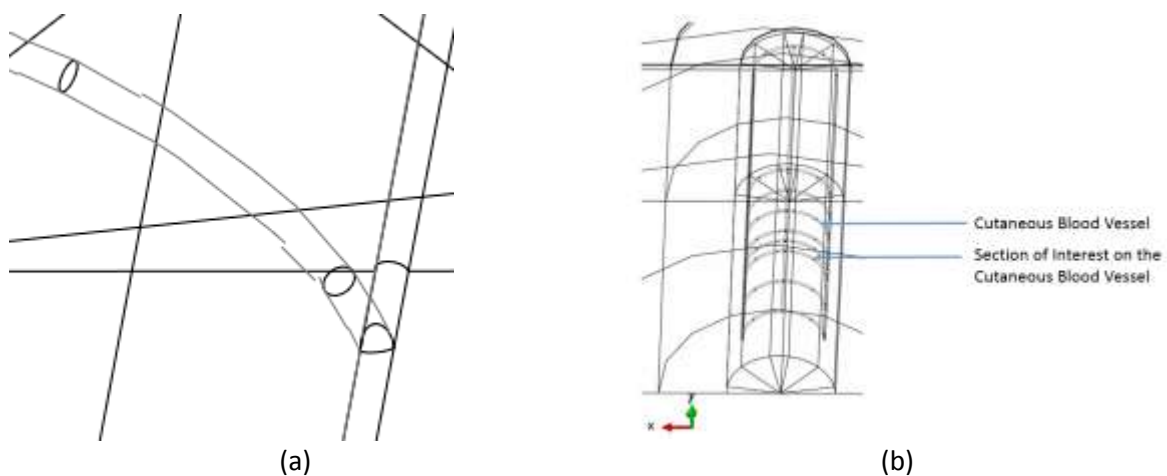


Figure 2 Cutaneous Blood Vessels and Points of Interest

Boundary Conditions

PUs often occur on soft tissue which has little muscle tissue therefore the cutaneous layers were assumed to be immovable in vertical direction and limited movement sideways when only pressure was applied. This assumption allowed the application of rigid boundary condition at the bottom face of the model as shown in Figure 3 to restrict any of the translational and rotational movement. This was indicative of PUs being most prevalent over bony prominences.

The other boundary condition was symmetric which was applied at the Z-Y plane of the model as shown in Figure 3. The applied symmetrical boundary condition reduced the computational simulation time but did not compromise the results.

The missing boundary condition was related to the circumference of the model. Any part of the human skin is surrounded by other similar mechanical property of materials. This poses some degree of restriction to the deformation of the skin at the centre. However, this incomplete restriction poses a difficulty to the computational modelling of the human skin. The deformation of the area of interest of the model (centre part of the model) would be affected significantly by the application of the boundary condition on the circumference. The method used to counter the difficulty posed by the accurate boundary conditions on the circumference was to enlarge the model which kept the circumference further away from the area of interest located at the centre of the model.

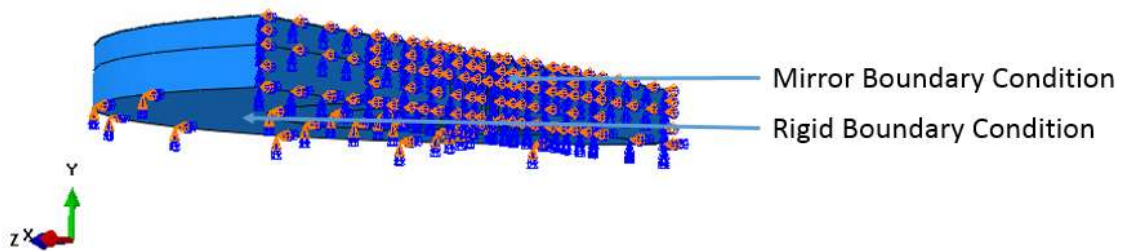


Figure 3 Application of Boundary Conditions

Mechanical Properties and Dimensions of the Cutaneous Layers

The respective mechanical properties were applied to the cutaneous layers in order to analyse the deformation of each of the cutaneous layers shown Table 1. These mechanical properties were usually acquired by means of in vivo suction or in vitro tensile test. Mechanical properties were selected from literature; the models' accuracy relies on the relative confidence in the mechanical properties presented. The distinct mechanical property of the wall of the blood vessels was assumed to be insignificant because of the relative negligible thickness compared to the rest of the cutaneous layers. In addition, the mechanical properties, acquired below included the influence of the presence of the cutaneous blood vessels. Hence, it is reasonable to assume that the mechanical properties of the wall of the cutaneous blood vessels could be neglected at this instance.

Table 1 Mechanical Properties and Dimensions of the Cutaneous Layers

		Values	References
Thickness of	Stratum Corneum	10 μm	(26, 27)
	Epidermis	42 μm	
	Dermis	1,285 μm	
	Hypodermis	1,913 μm	
Young's Modulus of	Stratum Corneum	1 MPa	(26)
	Epidermis	0.05 MPa	

	Dermis	0.6 MPa	
	Hypodermis	0.11 MPa	
Poisson's ratio of skin		0.5	(28)

Loading of the Model

The mechanical loading, pressure, was applied at the top surface of the model as indicated on Figure 1. The area of loading affects the deformation of the area of interest which is the middle radial section of the model. The deformation of the middle section was the key interest of the study. However, the deformation of the middle section increases with an increase of the loading area surrounding the middle section. Simulation test runs ensured that the deformation of the area of interest had minimum effect of the loading area by conducting the convergence test of the loading area against the reduction in the cross-sectional area of the cutaneous blood vessels. Only the middle radial section (radial section 1) was loaded in the first simulation test run and radial section 1 and 2 were loaded for the second simulation test run and so forth to the 8th simulation test run where radial section 1-8 were loaded. The effect area of loading was demonstrated by the convergence test.

In order to relate the computational data to a set of experimental data, the range of applied loading of the computational model was comparable to that used in the laser Doppler measurement. The loading to the computational model was in the range of 23.00 mmHg to 137.94 mmHg.

Acquisition of the Clinically Relevant Experimental Data

Clinically relevant data was an essential part of the study. This served as a tool for establishing the relationship between the computational model and the reality. It ensured the computational model was clinically relevant and fit to become a tool for medical device development as well as device performance prediction.

Laser Doppler Velocimetry PF5010- LDPM (Perimed) was utilised to measure the velocity of particulate red blood cells, within cutaneous blood flow velocity of the six volunteers. This was assumed to be an indicator of the cutaneous blood flow velocity. Different loads were applied to the probe of the laser Doppler velocimetry resulting in application of pressure to the back of the hands of the volunteers. The magnitudes of the loading were from 23.08 mmHg to 115.44 mmHg, comparable to that used in the computational model as 45mmhg was found to be sufficient to cause PUs in specific condition and 12 to 32mmHg were found to be the capillary pressure by Landis (29, 30) and further increase in load resulting in discomfort to the participants. Throughout the loading time, all six of the volunteers found the loadings to be acceptable with little discomfort experienced, the particular situation could be analogous to a cannular tube applying pressure to the back of a hand in a clinical situation or an oxygen mask being securely attached to the face.

The setup of the laser Doppler measurement is illustrated in Figure 4. The hand of a volunteer, pressure mapping sensor I-scan 5051 (Tekscan) and the probe of the laser Doppler were put in the fixture. The loads were applied by restricting the space inside the fixture and using the pressure sensor as an indicator of applied pressure. The cutaneous blood flow was monitored using the laser Doppler.

The pressure exerted was measured by the pressure mapping sensor while the laser Doppler provided arbitrary values of the blood flow velocity. An initial reading was acquired before exerting any pressure on the probe of the laser Doppler. Consequently, the change in the values provided by

the laser Doppler were calculated. The readings were taken at intervals of fifteen seconds for a duration of two-minutes. This was repeated for each magnitude of pressure applied to the hands of the volunteers. After each loading cycle, a two-minute settling period was provided in order to ensure the effect of the loadings was captured by the laser Doppler. The maximum and minimum values in each of the two-minute measuring period were discarded and the average of the remaining values were used to calculate the percentage change in the blood flow velocity.

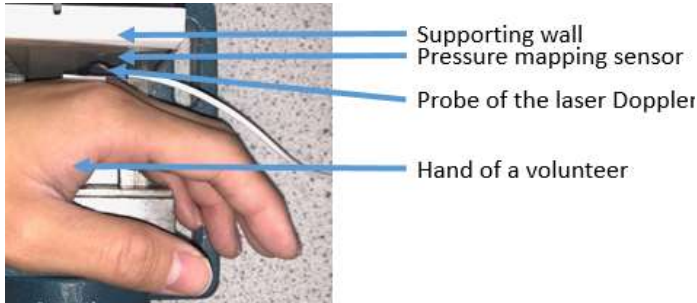


Figure 4 Setup of the Laser Doppler Measurement

Result

Loading Area Simulation Test Runs

The results of the simulation test runs are presented in Figure 5. There were eight simulation test runs in total and the loading areas were increased in each of the test runs. Only radial section 1 was loaded for the first test run, radial sections 1 and 2 were loaded for the second test run and until the last test run in which radial sections 1 to 8 were loaded. The data points on Figure 5 present the average percentage changes of the cross-sectional area of the sections of interest on the cutaneous blood vessels of the current model.

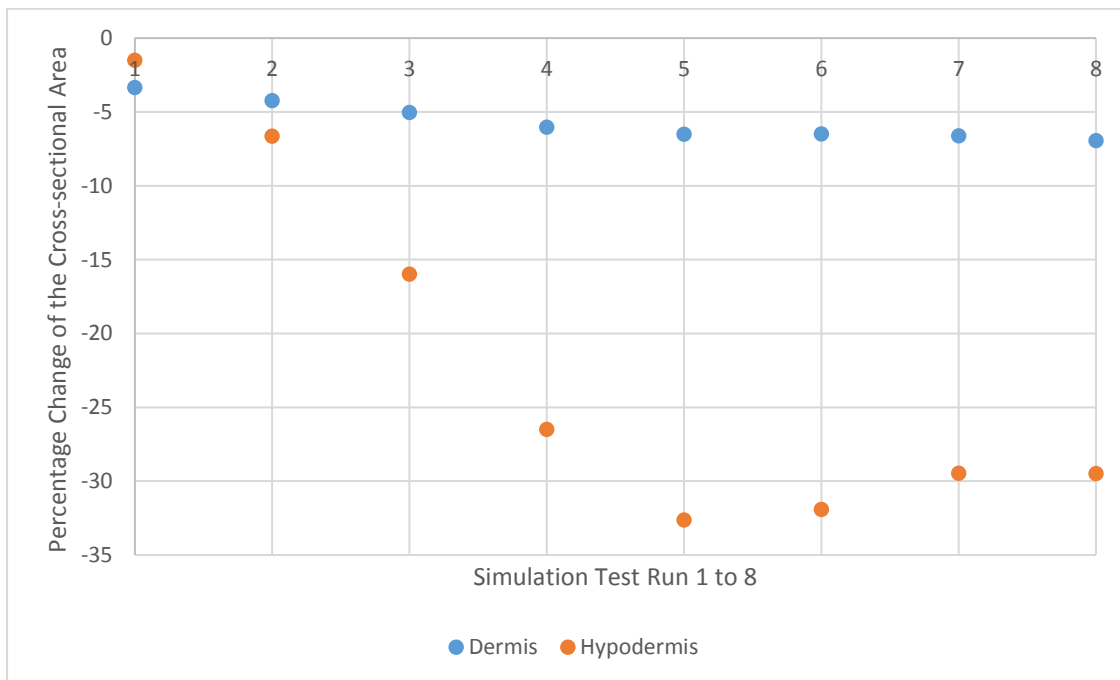


Figure 5 Percentage change of the cross-sectional area of blood vessels for 1st to 8th simulation test run

Figure 5 demonstrated the convergent trend of the data points where all the points converged to two values including approximately -6% and -30%. It was noticeable that less reductions were caused by the applied pressure for the cutaneous blood vessels located at the dermis layers as compared to those located at the hypodermis layer. All the points converged to -6% were located at dermis layers and the remaining points were located at hypodermis layers. Figure 5 also demonstrates that the data points started to be converged at the 7th simulation test run.

Change in the Cross-sectional Area by the Computational Model

The reduction in cross-sectional area on cutaneous blood vessels were calculated by the change in three-dimensional coordinates of the nodes on the cutaneous blood vessels of the developed model. The percentage changes of the cross-sectional area are shown in Figure 6. The grey-coloured points were the average all the 6 sections of interest in each of the 2 and 7 cutaneous blood vessels located at dermis and hypodermis respectively.

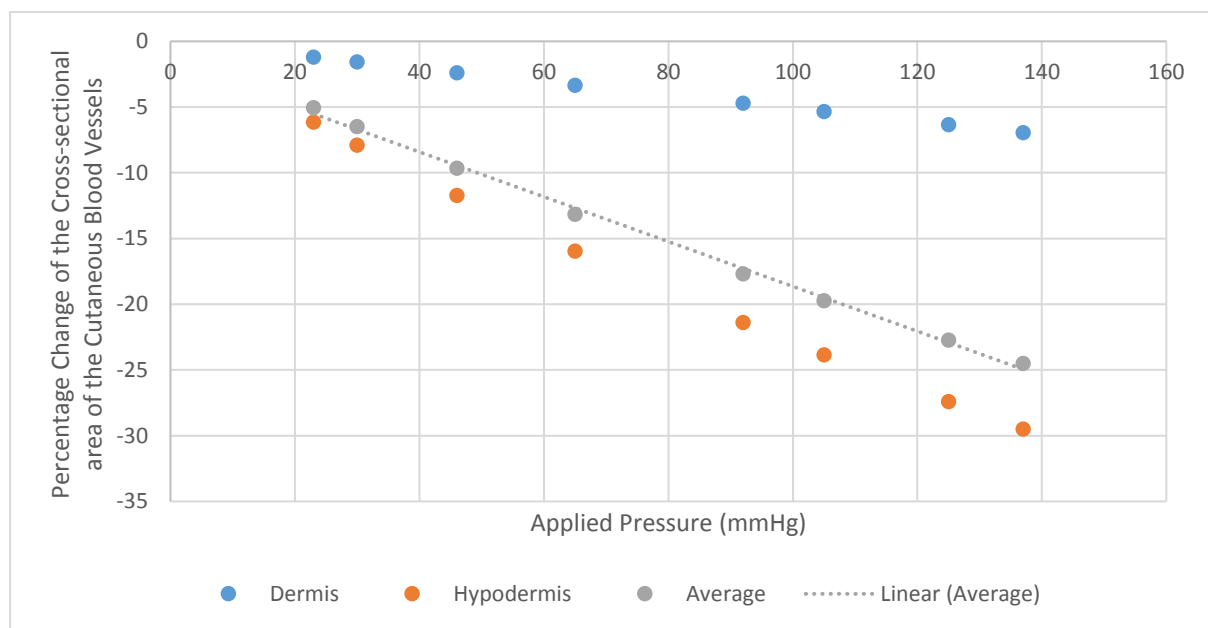


Figure 6 Percentage Change of the Cross-sectional Area of the Cutaneous Blood Vessels

Change in the Laser Doppler Readings

Six volunteers participated in the study aged between 24 years to 50 years. The average percentage change of the blood flow velocity of the six volunteers is shown in Figure 7. The data on the graph fitted a logarithmic curve.

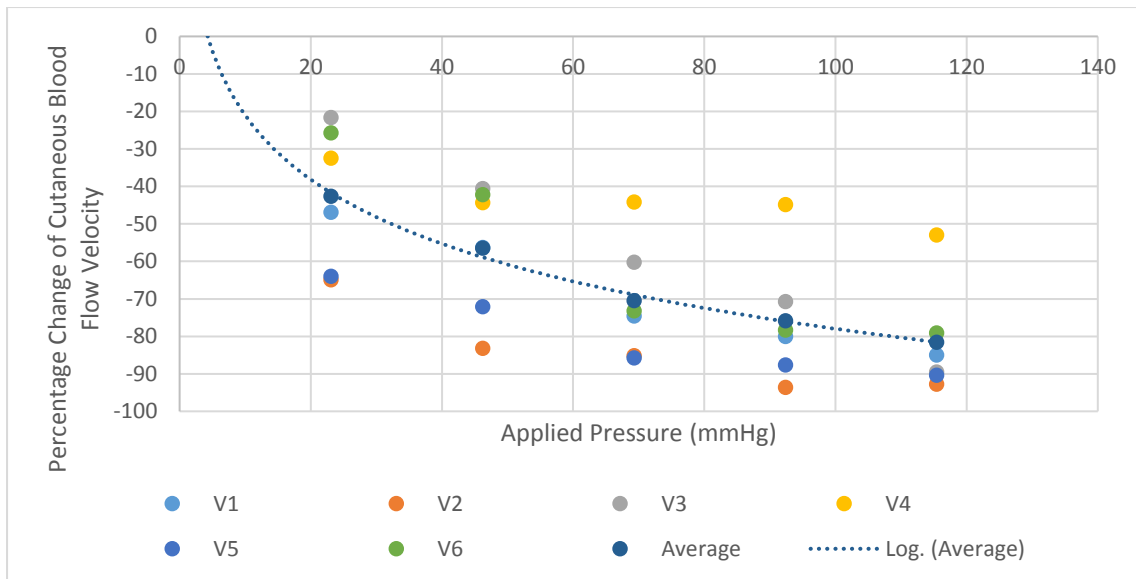


Figure 7 Percentage Change of the velocity of blood flow captured by Laser Doppler Velocimetry

Discussion

The percentage difference of the percentage change for the 7th and 8th simulation test runs was 0.38% in Figure 5. Therefore, section 1-7 were loaded for the model which minimise the effect of loading area of the magnitude of the deformation of the cutaneous blood vessels.

The percentage changes in the cross-sectional area of the sections of interest on the cutaneous blood vessels by the presented model were demonstrated by Figure 6. There were three sets of data including the dermis set, hypodermis set and the averaged set. The averaged set is utilised in later stage to compare with the experimental results of the clinically relevant experimental data. It showed that the cross-sectional area of the cutaneous blood vessels decreased linearly with the increase of the magnitudes of the applied pressure.

The percentage changes in the blood flow velocity measured by the laser Doppler were demonstrated by Figure 7. The backs of the volunteers' hands were loaded with 23.08 mmHg to 115.44 mmHg. Higher magnitudes of pressure were not applied to the volunteers as discomfort was caused. Although higher magnitudes of pressure could not be applied, the existing range of applied pressure covers a wide range of magnitudes of pressure commonly perceived in clinical practices. The blood flow velocity decreased with the increase with the magnitude of the applied pressure. A logarithm curve fitted through the data points acquired from the laser Doppler measurement. It was exceptionally hard to acquire steady data from the measurement. All the volunteers were required to remain still throughout the measurement period as any slight movement could cause abnormal peaks in the measured readings. The relationship between the changes in the blood flow velocity caused by the applied pressure was demonstrated Figure 7.

The relationship between the computational data and the clinically relevant experimental data is presented in Figure 8. The graph indicates that the cutaneous blood flow velocity decreases with the cross-sectional area of the cutaneous blood vessels. The FEA data represented the percentage change of the cross-sectional area of the blood flow domain, cutaneous blood vessel, while the experimental data represented the percentage change in the flow velocity.

According to fluid mechanics theory, Bernoulli's equation, for incompressible steady state flow, a reduction in flow area should result in an increase in flow velocity; this is not the case for the present example as demonstrated in figure 8. This is due to the complexities of the vascular system. Blood itself is a multiphase liquid and not expected to behave like a Newtonian fluid due to the complex physiology and pathology blood cells in which the red blood cells and blood plasma contribute to 45 and 55 percent of the whole blood respectively (31).

In addition to this, the vascular system would potentially allow for flow to be restricted and decreased in velocity in one area due to other areas of the vascular system - particularly where the focus of this study was cutaneous blood flow through smaller capillaries rather than arterial flow.

The Laser Doppler specifically measures flow of red blood cells, there is a possibility that because of the deformation of the cutaneous blood vessels, as demonstrated by the FEA model to be an average of 25% reduction, red blood cells are not able to pass through the restricted pathway therefore leading to ischemia.

Medical device developers or clinicians could utilise the presented computational model to determine the percentage change of the cross-sectional area of the cutaneous blood vessels and deducing the equivalent percentage change in the flow velocities by referring to Figure 8. The developed computational model and the established relationship could be used to evaluate the influence of mechanical loads on percentage change of the cutaneous blood flow velocity. This is typically useful for the case of understanding the effects of medical devices. This paper presents a method to convert an external parameter, interface pressure, to a physiological parameter, percentage change in cutaneous blood flow velocity. It allows a better understanding in clinical practice for the physical effects of medical devices to the likelihood of the formation of superficial pressure ulcers.

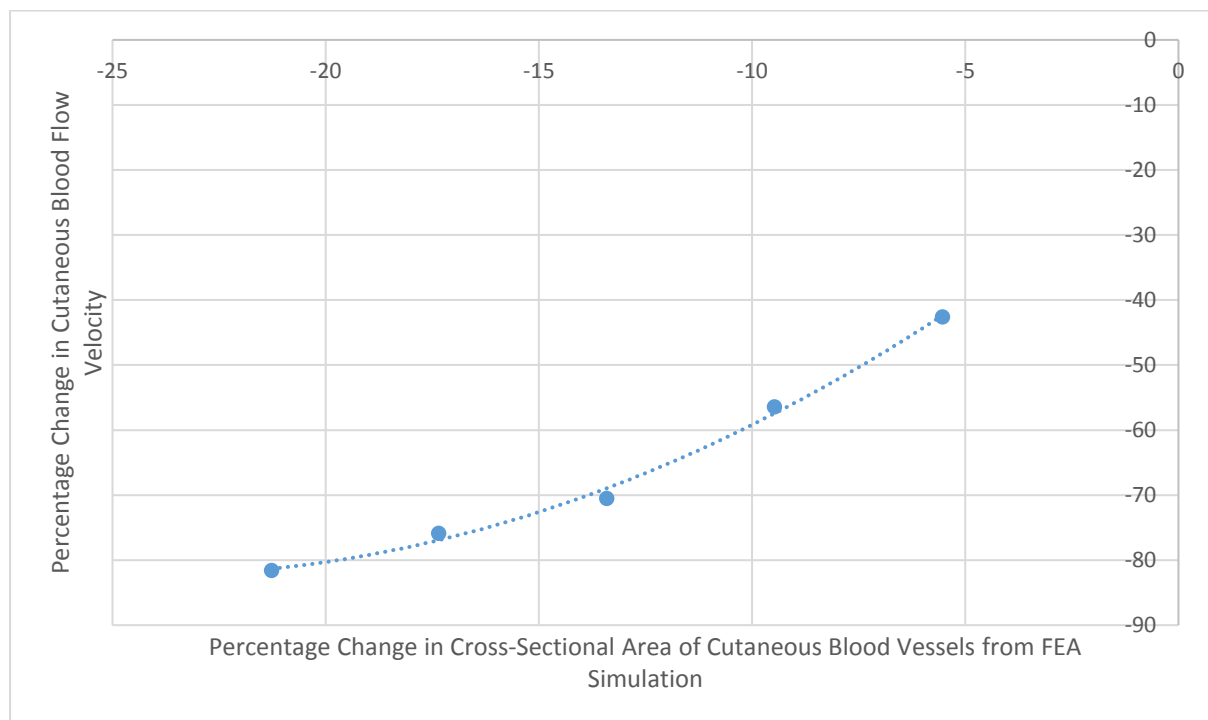


Figure 8 Relationship between Computational Data and Clinically Relevant Experimental Data

The healthy volunteer study sought to prove the feasibility in the methodology of relating the computational model to a set of clinically relevant experimental data and increase understanding

the change in blood flow caused by mechanical loads. The study presents the data and demonstrates the feasibility of such method as a pilot study. The computational model is useful in determining the behaviours of cutaneous layers and the change in the cross-sectional area of the cutaneous blood vessels. The computational model can approximate the change in the cross-sectional area of skin with different conditions for instance, different skin mechanical properties due to ageing and condition could be evaluated. A larger experimental study could seek to correlate this with further experimental data. The developed model and the established relationship could reduce further involvement in human participants for specific skin conditions by conducting computational simulations with different input, mechanical properties. This paper fills the gap which exists in provision of effective tools and experimental results to evaluate the cross-sectional area change and the blood flow velocity by developing a computational model and a feasible experimental methodology.

Conclusion

A three-dimensional computational model capable of demonstrating change in the cross-sectional area of the cutaneous blood vessels was developed. This can be a robust tool for medical device developers as well as an effective indicator for clinicians. A linear relationship of decrease percentage change of the cross-sectional area of the cutaneous blood vessels with the increase in the magnitude of the applied pressure was found. The logarithm relationship of decrease in the blood flow velocity with the increase in the applied pressure was also discovered by conducting laser Doppler measurement. A relationship was established between the computational data and the clinically relevant experimental data to ensure the developed model will be clinically relevant.

Acknowledgement

The authors gratefully acknowledge the UK's Engineering and Physical Sciences Research Council (EPSRC) funding of the EPSRC Centre for Innovative Manufacturing in Advanced Metrology (Grant Ref: EP/ IO33424/1).

References

1. Millington PF, Wilkinson R. Skin. Cambridge: Cambridge University Press; 2009.
2. Agency_for_Healthcare_Research_and_Quality USDoHHS. Preventing Pressure Ulcers in Hospitals, are we ready for this change? 2014 [updated October 2014; cited 2017 23rd Dec]. Available from: <https://www.ahrq.gov/professionals/systems/hospital/pressureulcertoolkit/putool1.html>.
3. Safety_Thermometer. ST Nati Safe Harm Tab Jul 2017 Jul 2018. NHS; 2018.
4. EPUAP&NPUAP EPUAPaNPUP. Prevention and treatment of pressure ulcers: quick reference guide. 2009.
5. NHS. Stop the pressure 2016 [cited 2017 9 May]. Available from: <http://nhs.stopthepressure.co.uk/>.
6. Bennett G, Dealey C, Posnett J. The cost of pressure ulcers in the UK. Age and Ageing. 2004;33(3):230-5.
7. Dealey C, Posnett J, Walker A. The cost of pressure ulcers in the United Kingdom. Journal of Wound Care. 2012;21(6):261-6.
8. Yusuf S, Okuwa M, Shigeta Y, Dai M, Iuchi T, Rahman S, et al. Microclimate and development of pressure ulcers and superficial skin changes. International Wound Journal. 2015;12(1):40-6.
9. Zhong W, Xing MMQ, Pan N, Maibach HI. Textiles and Human Skin, Microclimate, Cutaneous Reactions: An Overview. Cutaneous and Ocular Toxicology. 2006;25(1):23-39.

10. EPUAP N, PPIA. Prevention and Treatment of Pressure Ulcers: Clinical Practice Guideline. Western Australia; 2014.
11. Gefen A, van Nierop B, Bader DL, Oomens CW. Strain-time cell-death threshold for skeletal muscle in a tissue-engineered model system for deep tissue injury. *Journal of Biomechanics*. 2008;41(9):2003-12.
12. Linder-Ganz E, Engelberg S, Scheinowitz M, Gefen A. Pressure–time cell death threshold for albino rat skeletal muscles as related to pressure sore biomechanics. *Journal of Biomechanics*. 2006;39(14):2725-32.
13. Makhous M, Lim D, Hendrix R, Bankard J, Rymer WZ, Lin F. Finite Element Analysis for Evaluation of Pressure Ulcer on the Buttock: Development and Validation. *IEEE Transactions on Neural Systems and Rehabilitation Engineering*. 2007;15(4):517-25.
14. *Dictionary_of_Nursing*. ischaemia. 7 ed: Oxford University Press; 2017.
15. Bhattacharya S, Mishra RK. Pressure ulcers: Current understanding and newer modalities of treatment. *Indian journal of plastic surgery : official publication of the Association of Plastic Surgeons of India*. 2015;48(1):4-16.
16. Gefen A. Reswick and Rogers pressure-time curve for pressure ulcer risk. Part 1. *Nursing standard (Royal College of Nursing (Great Britain) : 1987)*. 2009;23(45):64-8.
17. Gefen A. Reswick and Rogers pressure-time curve for pressure ulcer risk. Part 2. *Nursing standard (Royal College of Nursing (Great Britain) : 1987)*. 2009;23(46):40-4.
18. Black JM, Cuddigan JE, Walko MA, Didier LA, Lander MJ, Kelpel MR. Medical device related pressure ulcers in hospitalized patients. *International Wound Journal*. 2010;7(5):358-65.
19. Linder-Ganz E, Shabshin N, Itzhak Y, Yizhar Z, Siev-Ner I, Gefen A. Strains and stresses in sub-dermal tissues of the buttocks are greater in paraplegics than in healthy during sitting. *Journal of Biomechanics*. 2007;41(3):567-80.
20. Levy A, Kopplin K, Gefen A. An air-cell-based cushion for pressure ulcer protection remarkably reduces tissue stresses in the seated buttocks with respect to foams: Finite element studies. *Journal of Tissue Viability*. 2013;23(1):13-23.
21. Luboz V, Bailet M, Grivot CB, Rochette M, Diot B, Bucki M, et al. Personalized modeling for real-time pressure ulcer prevention in sitting posture. *Journal of Tissue Viability*. 2017;27(1):54-8.
22. Savonnet L, Wang X, Duprey S. Finite element models of the thigh-buttock complex for assessing static sitting discomfort and pressure sore risk: a literature review. *Computer Methods in Biomechanics and Biomedical Engineering*. 2018;21(4):379-88.
23. Leung IPH, Fleming L, Walton K, Barrans S, Ousey K. Development of a model to demonstrate the effects of friction and pressure on skin in relation to pressure ulcer formation. *Wear*. 2017;376–377, Part A:266-71.
24. Démarchez M. Cutaneous vasculature [Webpage]. Michel Démarchez 2011 [updated 15 May 2011; cited 2016 1st August]. Available from: <http://biologiedelapeau.fr/spip.php?article21>.
25. Saladin K. *Human Anatomy* 2007 Ed 2007 Edition: Rex Bookstore, Inc.; 2007.
26. Lévêque JL, Audoly B. Influence of Stratum Corneum on the entire skin mechanical properties, as predicted by a computational skin model. *Skin Research and Technology*. 2013;19(1):42-6.
27. Hwang K, Kim H, Kim DJ. Thickness of skin and subcutaneous tissue of the free flap donor sites: A histologic study: Thickness of the Free Flap Donor Sites. *Microsurgery*. 2016;36(1):54-8.
28. Liang X, Boppart SA. Biomechanical Properties of In Vivo Human Skin From Dynamic Optical Coherence Elastography. *IEEE Transactions on Biomedical Engineering*. 2010;57(4):953-9.
29. Dinsdale SM. Decubitus ulcers: role of pressure and friction in causation. *Archives of Physical Medicine and Rehabilitation*. 1974;55(4):147-52.
30. Landis E. micro-injection studies of capillary blood pressure in human skin. *Heart: official journal of the british cardiac society*. 1930;15:209.

31. American_Society_of_Hematology. Blood Basics 2019 [Available from: <http://www.hematology.org/Patients/Basics/>].